ELSEVIER

Journal of Organometallic Chemistry 573 (1999) 36–46

Journal of Organometallic Chemistry

# Synthesis, structure and electrochemistry of ferrocenylethynylsilanes and their complexes with dicobalt octacarbonyl[1]

Noel W. Duffy, Brian H. Robinson, Jim Simpson *

*Department of Chemistry, University of Otago, P.O. Box 56, Dunedin, New Zealand*

Received 17 February 1998

**Abstract**

Coupling of lithium ethynylferrocene to alkyl and aryl chlorosilanes and to silicon tetrachloride leads to the formation of a variety of ferrocenylethynylsilanes, $[(\eta^5\text{-}C_5H_5)Fe(\eta^5\text{-}C_5H_4C_2)]_{4-n}SiR_n$ ($n = 0–3$, R = Me, Ph). An additional series of compounds $[(\eta^5\text{-}C_5H_5)Fe(\eta^5\text{-}C_5H_4C_2)]_{4-n}Si(n\text{-}Bu)_xR_y$ ($n = 0–3$, $x + y = n$, R = Me, Ph) result from competitive reactions of excess *n*-BuLi at the silicon centre. Dicobalt octacarbonyl reacts with the ferrocenylethynylsilanes to give dicobalt hexacarbonyl derivatives, but for the tris- and tetrakis-compounds coordination of $Co_2(CO)_6$ is limited to two of the alkyne units as a result of steric crowding around the silicon centre. The crystal and molecular structure of the complex $[(\eta^5\text{-}C_5H_5)Fe(\eta^5\text{-}C_5H_4C\text{–}(Co_2(CO)_6)C]_2Si[(C{\equiv}C\text{-}\eta^5\text{-}C_5H_4)Fe(\eta^5\text{-}C_5H_5)]_2$ has been determined from X-ray data. Electrochemical investigation of the ferrocenylethynylsilanes and their dicobalt complexes shows that the equivalent ferrocenyl redox centres in these molecules are non-interacting. 

*Keywords:* Ferrocenylethynyl-silanes; Dicobalt octacarbonyl; Alkynyls; Alkyne complexes

## 1. Introduction

Ferrocenylethynyl complexes have been shown [1–3] to provide viable templates for long range electronic communication between the ferrocene centres through bridging alkyne units. These systems have also been targeted for the production of non-linear optical materials as the oxidation state, redox behaviour and potential for metal–ligand or ligand–metal charge transfer of the metal centre can be changed, to tune the hyperpolarisability of the molecular systems [4]. In the field of multiple redox centre complexes, an interesting dichotomy has emerged concerning the role of silicon in augmenting or precluding electron transfer between redox active centres. Thus effective electronic interaction, evidenced by the observation of discrete oxidation peaks in cyclic voltammograms of compounds containing two or more equivalent ferrocene centres, has been demonstrated in silicon bridged dimers [5], silaferrocenophanes [6–8], oligomers [6] and some polymers [5,9–11]. Disilyl and trisilyl bridges also support interactions between equivalent ferrocene centres [1,12]. In contrast, the interpolation of silicon atoms between ferrocene and tricobalt carbon redox centres in 1,1′-$Fc'[SiR_2CCo_3(CO)_9]_2$ [13] or between two cluster centres and potentially conducting oxo or aromatic bridge units [14], effectively insulates the two equivalent redox centres.

The preparation of ferrocenylethynylsilanes reported herein offers an opportunity to investigate the ability of a central silicon atom to promote electron transfer when bound to an array of conjugated ferrocenylethynyl substituents. Similarly, the reaction of dicobalt octacarbonyl with these ferrocenylethynylsilanes gave dicobalt complexes with additional equivalent redox centres.

* Corresponding author.

[1] Dedicated to Professor Brian Johnson on the occasion of his 60th birthday.

0022-328X/99/$ - see front matter 
*PII* S0022-328X(98)00597-X

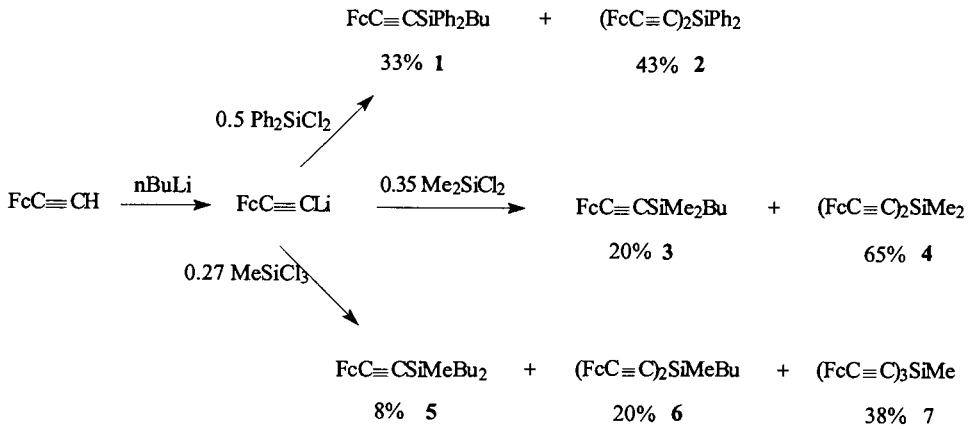


Scheme 1.

## 2. Results and discussion

### 2.1. Synthesis of ferrocenethynylsilanes

The ferrocenylethynyl derivatives, **1–11**, were prepared from FcC≡CLi[2] and the appropriate $SiR_xCl_{4-x}$; $x = 0–2$, R = Me, Ph (Schemes 1 and 2). The butyl-substituted products result from the small excess of *n*-BuLi effectively competing with the acetylide for a site on the silicon atom.

The problem of unwanted substitution at the silicon centre was alleviated by employing a noncoordinating nucleophilic base (LDA) with a 7:1 ratio of ethynylferrocene to silicon tetrachloride. This procedure gave analytically pure **11** as an orange solid in good yield without significant byproducts (Scheme 2).

The bis-**2** [15], **4** [15], **6**, **9**, tris-**7**, **10** and tetrakis-**11** ferrocenylethynyl derivatives were all stable orange solids, whereas the mono- **1**, **3**, **5** and **8** were dark orange oils. All compounds were characterised by elemental analysis, mass spectra, IR and NMR spectroscopy. Parent molecular ions were observed in high abundance in their mass spectra—an exception was **2** for which the highest peak was $[M\text{-}FcC{\equiv}C]^+$—and the primary fragmentation process involved cleavage of the central Si–C bond. Clearly defined $\nu$(C≡C) bands in the range 2148–2153 $cm^{-1}$ were the feature of the IR spectra. Assignments for the $^1H$- and $^{13}C$-NMR spectra were straightforward and detailed assignment for the butyl substituents of **1**, **3**, **5**, **6**, **8** and **9** was aided by DEPT, COSY and HETCOR pulse sequences (see Section 3). $^{13}C$ spectra show the resonances of the alkyne C atoms bound to the central Si to be significantly shielded ($\delta$ ca. 85–90 ppm) in comparison to those bound to the ferrocene moieties ($\delta$ ca. 105–109 ppm). $^{29}Si$-NMR spectroscopy [16,17] proved to be useful tool for characterising crude reaction products. Replacement of the phenyl substituents (in **1** and **2**) with methyl or butyl groups gave a downfield shift of ca. 7–8 or ca. 11–12 ppm, respectively; in contrast, exchanging butyl for methyl substituents results in a 3.9 ppm downfield shift. Chemical shift additivity was found in the series $R_{4-n}Si(C{\equiv}CFc)_n$, with a linear variation in chemical shift, the shielding per alkyne substituent being constant at ca. 24–25 ppm across the series.

Reaction of **1** and **3** with $Co_2(CO)_8$ gave the expected [18] products $\{FcC[Co_2(CO)_6]C\}SiPh_2Bu$ **12** and $\{FcC[Co_2(CO)_6]C\}SiMe_2Bu$ **13** in near quantitative yields. Similarly, the bis-compounds **2** and **4** gave good yields of the disubstituted clusters **16**, and **17** with only trace amounts of the monosubstituted **14** and **15** (Scheme 3). All these derivatives were isolated as green air-stable crystals.

Significantly, substitution by $Co_2(CO)_6$ occurred at only two –C≡C– units in the tris-alkyne **7** resulting in **19** (Scheme 4) with only trace amounts of the singly substituted complex **18**.

Likewise only the di-substituted product **20** was isolated from **11** and attempts to force further substitution using elevated temperatures resulted in decomposition. From the crystal structure of **20** vide infra, it is not difficult to see that there is insufficient space for a higher degree of substitution because of steric congestion about the central silicon atom. A tris-alkynyl complex $[MeC(Co_2(CO)_6C]_3SiH$ was isolated by Corriu [19] from the slow addition of $Co_2(CO)_8$ to a dilute solution of $(MeC{\equiv}C)_3SiH$. The decreased steric bulk of the methyl substituents and the effectively empty quadrant occupied by the H atom greatly reduce the congestion around the Si atom in this case. Even so, the resulting tris-complex had low thermal stability in solution.

Complexes **14–20** were characterised by elemental analysis, mass spectra and spectroscopy. Parent molecular ions were not generally observed in the mass spectra of the dicobalt complexes due to the facile loss of 1–3 carbonyl groups, a common observation for

[2] Fc = ($\eta^5$-$C_5H_5$)Fe($\eta^5$-$C_5H_4$).

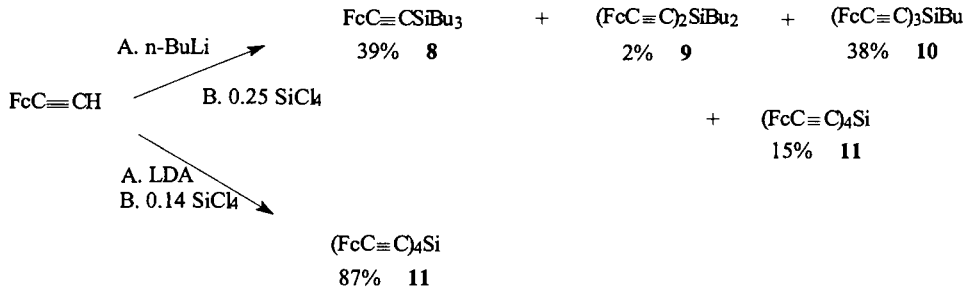


Scheme 2.

cobalt-carbonyl clusters. All clusters display the typical [18,20] $\nu$(CO) envelope of RCCR′$Co_2(CO)_6$ complexes, and for **19**, **20**, $\nu$(C≡C) bands in the IR spectra. Coordination of $Co_2(CO)_6$ to the alkyne results in a significant downfield shift in the alkyne $^{13}C$ resonances ($\delta$ ca. 128 ppm) and an average downfield shift of 16–20 ppm per cluster substituent in the $^{29}Si$ resonance, relative to the parent silane.

### 2.2. X-ray structure of $(FcC(Co_2(CO)_6C)_2Si(C{\equiv}CFc)_2$ **20**

Selected bond length and angle data for **20** are given in Table 1. A perspective view of the molecule in Fig. 1 defines the atom numbering scheme and shows only one of the two disordered conformations of the C(17)–C(110) cyclopentadiene ring. There are no molecular contacts not involving hydrogen atoms at $< 3.00$ Å; the shortest non-hydrogen atom contact is 3.05(1) Å between O(211) and O(411) ($x$, $y+1$, $z$) [21].

Fig. 1 shows the crystal structure of **20**, showing the atom numbering scheme. For clarity only numbering for the oxygen atoms of carbonyl ligands (the carbon atoms have the same number) and first two C atoms of consecutively numbered cyclopentadiene rings is shown in this diagram.

The molecule consists of a central silicon atom bound to four C≡C–Fc units. Two of the alkyne groups are coordinated to $Co_2(CO)_6$ fragments in a perpendicular fashion to form typical pseudo-tetrahedral $\mu_2$-$C_2Co_2$ units. In each $C_2Co_2$ unit the C≡C vector is approximately perpendicular to the Co–Co bond (interline angles Co(1)–Co(2)/C(1)–C(2) 88.9(7)°, Co(3)–Co(4)/C(3)–C(4) 87.6(6)° [22]. The $\mu_2$-$C_2Co_2(CO)_6$ units point away from one another to minimise repulsion between the cobalt bound carbonyl ligands. Each cobalt atom adopts a pseudo-octahedral coordination environment [22] defined in this structure by the carbyne C atoms, one axial and two equatorial carbonyl ligands and the 'bent' Co–Co bonds [23]. The coordination octahedra of the bound Co atoms share a common face. The equatorial carbonyl ligands adopt a classical 'sawhorse' arrangement [24] and are eclipsed when viewed down the respective Co–Co vectors.

The two independent Co–Co distances Co(1)–Co(2) 2.464(3) Å and Co(3)–Co(4) 2.459(3) Å are in the range found for metal–metal distances in related systems [25], and all of the Co–$C_{alkyne}$ distances are equal within experimental error (average 1.97(1) Å). Anticipated [26] differences in these parameters due to the asymmetrical environments of the cobalt bound carbyne C atoms are not revealed in this structure, perhaps reflecting the high estimated SD's on these parameters, resulting from the relatively weak data and disorder in the structure.

Bond lengths and angles within each of the ferrocenyl fragments are unremarkable and each pair of $\mu_5$-cyclopentadiene rings is almost parallel (interplanar angles C(11)–C(15)/C(16a)–C(110) 5(1)°; C(21)–C(25)/C(26)–C(210) 3.3(7)°, C(31)–C(35)/C(36)–C(310) 2(1)°; C(41)–C(45)/C(46)–C(410) 2(1)°). The two uncomplexed alkyne fragments are essentially linear, Si(1)–C(5)–C(6) 175(1), C(31)–C(6)–C(5) 175(1); Si(1)–C(7)–C(8) 176(1), C(41)–C(8)–C(7) 177(1). In contrast, the angles subtended by the ferrocene and silicon substituents at the alkyne C atoms highlight the *cis*-bent configuration of the coordinated alkynes, [Si(1)–C(1)–C(2) 150(1)°, Si(1)–C(3)–C(4) 151(1)°, C(11)–C(2)–C(1) 138(1), C(21)–C(4)–C(3) 144(1)°]. The widening of the angles to the Si substituents and a significant opening of the C(1)–Si(1)–C(3) angle to 116.3(5), compared to the other angles at Si(1) which average 108.1 (6)°, undoubtedly reflect the steric requirements of the two $\mu_2$-$C_2Co_2(CO)_6$ cores.

### 2.3. Redox chemistry of the ferrocenylethynylsilanes

Electrochemical data are given in Table 2. Ethynylferrocene, FcC≡CPh and FcC≡C$SiMe_3$, investigated as reference compounds, exhibit the typical reversible one-electron couple $[Fc]^{+\backslash 0}$ in their voltammetry. The electron-deficient alkyne Cp ring substituent gives an anodic shift of $[Fc]^{+\backslash 0}$ relative to ferrocene ($\Delta E^0 = 0.14$ V), whereas it is relatively insensitive to the substituent on the alkyne.

Fig. 2 shows the cyclic voltammogram responses for **7** which is representative of those for **2**, **4**, and **11**. Each voltammogram shows a single reversible Nernstian process A\B, $E^0 = 0.65 \pm 0.02$ V and linear plots of $I_p^a$ vs.

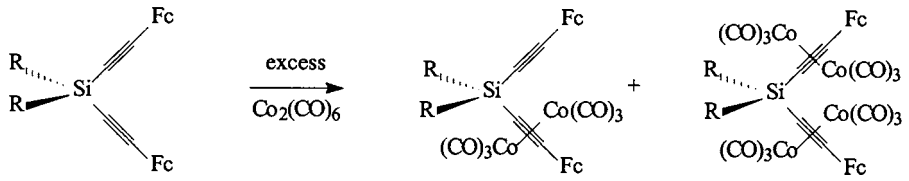


R = Ph **2** **14** **16**

R = Me **4** **15** **17**

Scheme 3.

$v^{1/2}$. Peak current ratios for $(FcC{\equiv}C)_2SiR_2$, **2** and **4**, relative to an equimolar concentration of in situ ferrocene clearly indicate a two-electron transfer; three-electron for **7** and 3.5-electron transfer for **11**, with the shape of a one-electron process. A respective two and three electron transfer was confirmed for **2** and **7** by coulometric methods.

The ratio of the diffusion currents $D_p/D_m$ for the series $(FcC{\equiv}C)_{4-n}SiR_n$ are estimated [27] for $n = 2$, 3, 4 to be 1.0, 0.9 and 0.75, respectively.

For the general case of molecules containing n non-interacting identical centres the successive electron transfers will follow simple statistics and the voltammogram will have the form of a one-electron process but with the magnitude determined by the number of electroactive centres. Clearly this is the situation for **2**, **4**, **7** and **11**. This result should be seen in the context of the interaction found in related compounds (Table 2) as measured by the difference in potential between two discrete ferrocenyl redox centres. Interpolation of one or more silicon atoms or alkyne units between two equivalent ferrocenyl units retains a degree of interaction but it is attenuated as the separation increases. Hence at **2**, **4**, **7** and **11**, the combination of the interposition of a silicon atom and an alkyne unit reduces the degree of interaction to a point where the redox processes differ by no more than a small statistical factor (Table 3).

Addition of a $Co_2(CO)_6$ group across the triple bond incorporates a reducible centre. Consequently, the oxidative electrochemistry of **14–20** was similar to that of the precursor silane. A typical cyclic voltammogram is shown in Fig. 3. The reversible couple **A**/**B** is obviously due to the noninteracting ferrocenyl centres ($E^{0\prime} = 0.61$ V, $AE_p = 91$ mV). Exhaustive oxidation at 0.7 V required approximately two mol equivalent of electrons per mol of **16**. **U** ($E_p$ ca. $-1.1$ V) can be assigned to reduction of both $C_2Co_2(CO)_6$ centres. As anticipated [2,32] the reduction process leads to series of fast ECE reactions, following radical anion formation, resulting in the formation of $Co(CO)_4^-$, oxidised at **V** ($E_p$ ca. 0.21 V). The ratio of peak currents $I_p(\mathbf{U})/I_p(\mathrm{A})$ ca. 1 on the initial anodic scan and ca. 1.5 on the cathodic scan.

Compound **20** has six redox centres with three different environments (two types of ferrocenyl moieties-adjacent to the substituted and unsubstituted alkynes respectively-and the $C_2Co_2(CO)_6$ centres). Two reversible oxidation processes, **A**/**B** at $E^{0\prime} = 0.61$ V and **C**/**D** at $E^{0\prime} = 0.68$ V, and an irreversible reduction (**U** at $E_p = -1.1$ V) are observed in the cyclic voltammogram (Fig. 4).

Resolution of the processes **A**/**B** and **C**/**D** is difficult using cyclic or square wave voltammetry. The difference in potential between **A**/**B** and **C**/**D** is similar to the difference between the principal couples for $FcC(Co_2(CO)_6)CH$ (0.54 V) and $FcC{\equiv}CH$ (0.61 V) suggesting that electron transfer processes at **A**/**B** and **C**/**D** are in the same sequence.

### 2.4. Conclusion

It is clear that the $SiC{\equiv}C$ moiety acts as an insulator in contrast to communication between ferrocenyl groups being facilitated by Si–Si. An important factor will be the character of the HOMO and LUMO of the link compared to those for ferrocene and this is being investigated in our laboratories. The observation that the tight space quadrant around the internal silicon restricts coordination to the alkyne groups may well be exploited to encourage through space, rather than through bond, interaction.

## 3. Experimental

All reactions were carried out in oven-dried glassware under an atmosphere of argon or oxygen-free nitrogen. Separation of reaction products by preparative thin layer chromatography (TLC) was often difficult due to similar $R_f$ values. In these cases repeated column or plate chromatography was employed; silica gel 60 was used exclusively. Ethynylferrocene was prepared from acetylferrocene by direct [33] and indirect [34] methods. Dichlorodimethylsilane, dichlorodiphenylsilane, methyltrichlorosilane and silicon [IV] chloride were purchased from Aldrich. Silicon [IV] chloride, dichlorodimethyl and methyltrichlorosi-

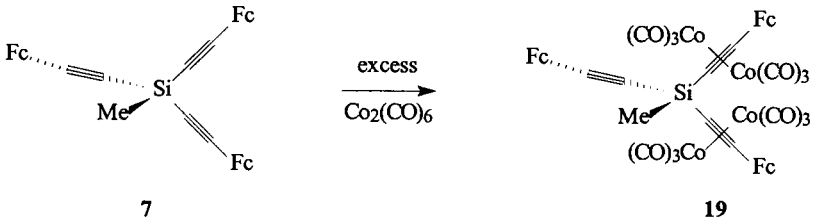


**7** **19**

Scheme 4.

lane were distilled prior to use. IR spectra were recorded on a Digilab FX60 spectrometer and NMR on a Varian VXR300 MHz or Gemini 200 MHz spectrometers. Microanalyses were carried out by the Campbell Microanalytical Laboratory, University of Otago. FAB mass spectra were recorded on a Kratos MS80RFA instrument with an Iontech ZN1 1NF atom gun. Electrochemical measurements were performed with a three-electrode cell using a computer controlled EG & G PAR 273A potentiostat/galvanostat at scan rates 0.05–10 V $s^{-1}$. A polished Pt disc electrode was employed; the reference was SCE uncorrected for junction potentials ([ferrocene]$^{+/0}$, was $E_{1/2} = 0.466$ V in acetone), the supporting electrolyte 0.1 M (TEAP) and the substrate ca. $1 \times 10^{-3}$ M.

The equation [27] $i_n(\theta) = ni_1(\theta)(D_p/D_m)^{1/2}$, where $i_1(\theta) = 4.9$ μA and $i_n(\theta)$ measured under identical conditions, was used to calculate diffusion coefficient ratios.

### 3.1. Preparation of $[(\eta^5\text{-}C_5H_5)Fe(\eta^5\text{-}C_5H_4C_2)]_xSi(C_6H_5)_2[CH_3(CH_2)_3]_{2-x}$: $x = 1, 2$

To a solution of FcC≡CH 1.75 mmol, 0.367 g) in dry THF (30 $cm^3$), at −78°C was added *n*-BuLi (1.1 equivalent, 1.2 $cm^3$ of 1.6 M in hexanes). Dichlorodiphenylsilane (0.88 mmol, 0.2 $cm^3$) was added at −78°C after 30 min. The mixture was warmed to r.t. over 30 min then stirred for two hours. The reaction mixture was hydrolysed at −5°C and extracted with dichloromethane. The organic layer was washed with distilled water and then dried over magnesium sulfate. The solvent was removed yielding yellow oil. Flash chromatography eluting with dichloromethane:hexane (1:10) yielded two product bands. The second band was removed using a 50:50 solvent ratio.

Band 1, orange **1**, $(\eta^5\text{-}C_5H_5)Fe(\eta^5\text{-}C_5H_4C_2)Si(C_6H_5)_2(CH_2CH_2CH_2CH_3)$, 33% Anal Calcd for $C_{28}H_{28}SiFe$: C, 74.99; H, 6.29; Found C; 75.21, H, 6.45, m.p. 46°C. $^1$H-NMR: ($CDCl_3$) δ 1.26 (t, 3H, $CH_3$), 1.45–1.65 (m, 6H $(CH_2)_3$) 4.27 (m, 2H, $C_5H_4$), 4.59 (m, 2H, $C_5H_4$); 4.28 (s, 5H, $C_5H_5$); 7.44–7.77 (m, 10H, $C_6H_5$). $^{13}$C-NMR ($CDCl_3$) δ 11.12, 13.8, 26.2, 26.4 ($C_4H_9$) 62.3q, 69.0 ($C_5H_4$), 72.1, 70.2 ($C_5H_5$), 128, 129.6, 134.8, 135.2q ($C_6H_5$). $^{29}$Si-NMR: ($CDCl_3$) δ −23.05. IR (KBr disk) ν(C≡C) 2151 $cm^{-1}$.

Band 2 orange **2** $[(\eta^5\text{-}C_5H_5)Fe(\eta^5\text{-}C_5H_4C_2)]_2Si(C_6H_5)_2$ [15], 42%, Anal Calcd for $C_{36}H_{28}SiFe_2$: C, 70.02; H, 4.70; Found C; 71.10, H, 5.07, m.p. 170°C. $^1$H-NMR: ($CDCl_3$) δ 4.27 (m, 4H, $C_5H_4$), 4.60 (m, 4H, $C_5H_4$); 4.29 (s, 10H, $C_5H_5$); 7.48, 7.94 (m, 10H, $C_6H_5$). $^{13}$C-NMR ($CDC_3$) 0 63.8q, 69.2, 72.2, ($C_5H_4$), 70.2 ($C_5H_5$), 84.6, 108.5 (C≡C), 128.2, 130.1, 134.0, 134.9(Ph). $^{29}$Si-NMR: ($CDCl_3$) δ −48.7. IR (KBr disk) ν(C≡C) 2149 $cm^{-1}$.

### 3.2. Preparation of $[(\eta^5\text{-}C_5H_5)Fe(\eta^5\text{-}C_5H_4C_2)]_xSi(CH_3)_2[(CH_2)_3CH_3]_{2-x}$: $x = 1, 2$

*n*-BuLi (1.1 equivalent, 1.6 M in hexane) was added to a solution of FcC≡CH (2.0 mmol, 0.42 g) in dry THF (20 $cm^3$) at −78°C. $Me_2SiCl_2$ (0.7 mmol) was slowly added after stirring for 1 h at −78°C. The mixture was stirred for 15 min before warming to −30°C and stirred for a further 15 min then to r.t.. Hydrolysis at −10°C followed by workup yielded a light yellow oil. TLC indicated three products. Flash chromatography separated two fractions. Band 1 orange oil, **3**, $(\eta^5\text{-}C_5H_5)Fe(\eta^5\text{-}C_5H_4C_2)Si(CH_3)_2(CH_2)_3CH_3$), 20%. Anal Calcd for $C_{18}H_{24}SiFe$: C, 66.66; H, 7.46; Found C; 66.87, H, 7.51. $^1$H-NMR: ($CDCl_3$) δ 0.21 ($J_{Si-H} = 7.5$ Hz, 6H, $Si(CH_3)_2$) 0.69 (t, 3H, $CH_3$) 0.95, 1.43 (m, 6H $(CH_2)_3$) 4.19 (m, 2H, $C_5H_4$), 4.45 (m, 2H, $C_5H_4$); 4.21 (s, SH, $C_5H_5$). $^{13}$C-NMR ($CDCl_3$) δ −1.36 ($CH_3$) 13.9, 16.15, 26.2, 26.3 ($C_4H_9$) 65.0q, 68.7, 71.8, ($C_5H_4$), 70.2 ($C_5H_5$), 89.92, 104.6 (C≡C). $^{29}$Si-NMR: ($CDCl_3$) δ −16.4. IR (KBr disk) ν(C≡C) 2148 $cm^{-1}$. Band 2 orange, **4**, $[(\eta^5\text{-}C_5H_5)Fe(\eta^5\text{-}C_5H_4C_2)]_2Si(CH_3)_2$ [15], 65%. *m/e* 475($M^+$); Anal Calcd for $C_{26}H_{24}SiFe_2$: C, 65.57; H, 5.08; Found C; 65.70, H, 5.19, m.p. 138°C. $^1$H-NMR: ($CDCl_3$) δ 0.44 ($J_{Si-H} = 7.1$ Hz, 6H, $Si(CH_3)_2$), 4.20 (m, 4H, $C_5H_4$), 4.49 (m, 4H, $C_5H_4$); 4.24 (s, 10H, $C_5H_5$). $^{13}$C-NMR ($CDCl_3$) δ 0.98 ($CH_3$) 64.3q, 68.96, 71.9, ($C_5H_4$), 70.24 ($C_5H_5$), 87.8, 105.2 (C≡C). $^{29}$Si-NMR: ($CDCl_3$) δ −40.6. IR (KBr disk) ν(C≡C) 2148 $cm^{-1}$.

Table 1
Selected bond lengths [A] and angles [°] for **20**

| | | | |
|---|---|---|---|
| Si(1)–C(1) | 1.826(13) | C(3)–C(4) | 1.33(2) |
| Si(1)–C(3) | 1.826(13) | Co(3)–Co(4) | 2.459(3) |
| Si(1)–C(5) | 1.794(13) | C(3)–Co(3) | 1.971(11) |
| Si(1)–C(7) | 1.783(13) | C(3)–Co(4) | 1.984(13) |
| C(1)–C(2) | 1.34(2) | C(4)–Co(3) | 2.005(12) |
| Co(1)–Co(2) | 2.464(3) | C(4)–Co(4) | 1.952(12) |
| C(1)–Co(1) | 1.972(11) | C(4)–C(21) | 1.45(2) |
| C(1)–Co(2) | 1.993(12) | Co(3)–C(311) | 1.82(2) |
| C(2)–Co(1) | 1.973(12) | C(311)–O(311) | 1.135(14) |
| C(2)–Co(2) | 1.962(12) | Co(3)–(:~(312) | 1.78(2) |
| C(2)–C(11) | 1.46(2) | C(312)–O(312) | 1.14(2) |
| Co(1)–C(111) | 1.86(2) | Co(3)–C(313) | 1.78(2) |
| C(111)–O(111) | 1.10(2) | C(313)–O(313) | 1.14(2) |
| Co(1)–C(112) | 1.77(2) | Co(4)–C(411) | 1.78(2) |
| C(112)–O(112) | 1.155(14) | C(411)–O(411) | 1.16(2) |
| Co(1)–C(113) | 1.76(2) | Co(4)–C(412) | 1.79(2) |
| C(113)–O(113) | 1.184(14) | C(412)–O(412) | 1.15(2) |
| Co(2)–C(211) | 1.79(2) | Co(4)–C(413) | 1.81(2) |
| C(211)–O(211) | 1.15(2) | C(413)–O(413) | 1.14(2) |
| Co(2)–C(212) | 1.79(2) | C(5)–C(6) | 1.21(2) |
| C(212)–O(212) | 1.14(2) | C(6)–C(31) | 1.43(2) |
| Co(2)–C(213) | 1.80(2) | C(7)–C(8) | 1.21(2) |
| C(213)–O(213) | 1.15(2) | C(8)–C(41) | 1.47(2) |
| C(1)–Si(1)–C(3) | 116.3(5) | O(213)–C(213)–Co(2) | 178.3(14) |
| C(5)–Si(1)–C(1) | 106.6(6) | C(4)–C(3)–Si(1) | 151.5(10) |
| C(5)–Si(1)–C(3) | 108.4(6) | C(3)–C(4)–C(21) | 143.5(12) |
| C(7)–Si(1)–C(1) | 108.4(6) | C(312)–Co(3)–C(311) | 103.2(6) |
| C(7)–Si(1)–C(3) | 108.3(6) | C(313)–Co(3)–C(311) | 105.4(6) |
| C(7)–Si(1)–C(5) | 108.8(6) | C(312)–Co(3)–C(313) | 98.9(6) |
| C(2)–C(1)–Si(1) | 149.8(10) | O(311)–C(311)–Co(3) | 176.8(14) |
| C(1)–C(2)–C(11) | 138.4(12) | O(312)–C(312)–Co(3) | 177.9(12) |
| C(112)–Co(1)–C(111) | 98.0(6) | O(313)–C(313)–Co(3) | 178.3(13) |
| C(113)–Co(1)–C(111) | 105.4(6) | C(411)–Co(4)–C(412) | 100.7(7) |
| C(113)–Co(1)–C(112) | 98.7(6) | C(411)–Co(4)–C(413) | 105.1(7) |
| O(111)–C(111)–Co(1) | 178.6(13) | C(412)–Co(4)–C(413) | 98.0(7) |
| O(112)–C(112)–Co(1) | 179.1(12) | O(411)–C(411)–Co(4) | 176.3(13) |
| O(113)–C(113)–Co(1) | 177.9(11) | O(412)–C(412)–Co(4) | 177.4(12) |
| C(211)–Co(2)–C(212) | 97.7(6) | O(413)–C(413)–Co(4) | 177.9(14) |
| C(211)–Co(2)–C(213) | 108.2(7) | C(6)–C(5)–Si(1) | 175.4(12) |
| C(212)–Co(2)–C(213) | 98.5(7) | C(5)–C(6)–C(31) | 174.7(13) |
| O(211)–C(211)–Co(2) | 175.1(13) | C(8)–C(7)–Si(1) | 175.6(13) |
| O(212)–C(212)–Co(2) | 174.6(13) | C(7)–C(8)–C(41) | 177.3(14) |

### *3.3. Preparation of $[(\eta^5\text{-}C_5H_5)Fe(\eta^5\text{-}C_5H_4C_2)]_xSi(CH_3)l(CH_2)_3CH_3]_{3-x}$: x = 1, 2, 3*

*n*-BuLi (1.1 equivalent, 1.1 M in hexane) was added slowly to a solution of FcC≡CH (7.15 mmol, 1.5 g) in dry THF (80 $cm^3$) at −78°C and stirred for 1 h. Methyltrichlorosilane (1.9 mmol, 0.284 g) was added slowly to maintain the temperature below −70°C. After stirring for 20 min the reaction mixture was slowly brought to r.t.. The reaction was quenched by hydrolysis at −5°C, extracted with dichloromethane and dried. Removal of the solvent yielded a dark orange oil. TLC (eluting 90 toluene: 10 ether) showed three products. One product crystallised from the mixture and was recrystallised from benzene/pentane to give fine yellow platelets of **7**, $[(\eta^5\text{-}C_5H_5)Fe(\eta^5\text{-}C_5H_4C_2)]_3SiCH_3$, 20%. *m/e* 670 ($M^+$); Anal Calcd for $C_{37}H_{30}SiFe_3$: C, 66.30; H, 4.51; Found C; 66.09, H, 4.20, m.p. >220°C. $^1$H-NMR: ($CDCl_3$) $\delta$ 0.61 ($J_{Si-H}$ = 7.2 Hz, 3H, $SiCH_3$), 4.21 (m, 6H, $C_5H_4$), 4.54 (m, 6H, $C_5H_4$); 4.26 (s, 15H, $C_5H_5$). $^{13}$C-NMR ($CDCl_3$) $\delta$ 2.12 ($CH_3$) 63.8q, 69.2, 72.0, ($C_5H_4$), 70.3 ($C_5H_5$), 85.6, 105.8 (C≡C). $^{29}$Si-NMR: ($CDCl_3$) $\delta$ −65.9. IR (KBr disk) $\nu$(C≡C) 2153 $cm^{-1}$.

The remaining oil was separated using TLC with pentane: diethyl ether (96:4) to yield two fractions. Band 1, orange oil, **5** $[(\eta^5\text{-}C_5H_5)Fe(\eta^5\text{-}C_5H_4C_2)]^-Si(CH_3)[(CH_2)_3CH_3]_2$, 3%. $^1$H-NMR: ($CDCl_3$) $\delta$ 0.16 ($J_{Si-H}$ = 7.0 Hz, 3H, $SiCH_3$ 0.66 (t, 3H, $CH_3$) 0.93, 1.38–1.45 (m, 6H $(CH_2)_3$) 4.17 (m, 2H,$C_5H_4$), 4.44 (m, 2H, $C_5H_4$); 4.19 (s, 5H, $C_5H_5$). $^{29}$Si-NMR: ($CDCl_3$) $\delta$ −17.7. Band 2, orange, **6**, $[(\eta^5\text{-}C_5H_5)Fe(\eta^5\text{-}C_5H_4C_2)]_2Si(CH_3)[(CH_2)_3CH_3]$, 4%. *m/e* 518 ($M^+$), Anal Calcd for $C_{29}H_{30}SiFe_2$: C, 67.20; H, 5.83; Found C, 67.52, H, 5.79, m.p. 146°C. H-NMR: ($CDCl_3$) $\delta$ 0.41 ($J_{Si-H}$ = 7.2 Hz, 6H, $Si(CH_3)_2$) 0.86 (t, 3H, $CH_3$) 1.01, 1.42–1.60 (m, 6H $(CH_2)_3$) 4.20 (m, 4H, $C_5H_4$), 4.50 (m, 4H,$C_5H_4$); 4.26 (s, 10H, $C_5H_5$). $^{13}$C-NMR ($CDCl_3$) $\delta$ 0.72 ($CH_3$) 13.95, 16.3, 26.0, 26.1 ($C_4H_9$) 64.4q, 68.7, 71.9, ($C_5H_4$), 70.21 ($C_5H_5$), 87.1, 105.5 (C≡C). $^{29}$Si-NMR: ($CDCl_3$) $\delta$ −41.4. IR (KBr disk) $\nu$(C≡C) 2150 $cm^{-1}$.

### *3.4. Preparation of $[(\eta^5\text{-}C_5H_5)Fe(\eta^5\text{-}C_5H_4C_2)]_{4-x}Si[(CH_2)_3CH_3]_x$: x = 0, 1, 2, 3*

*n*-BuLi (1.1 equivalent, 1.6 M in hexane) was added slowly to a solution of FcC≡CH (4.1 mmol, 0.863 g) in dry THF (60 $cm^3$) at −78°C. Silicon tetrachloride (1 mmol, 0.17 g) was added once an orange precipitate had formed and stirred for 30 min. Hydrolysis at 0°C followed by workup yielded a yellow oil which partially dissolved in ether leaving an orange solid, 11 (33%). *m/e* 864 ($M^+$); Anal Calcd for $C_{48}H_{36}SiFe_4$: C, 66.71; H, 4.20; Found C; 66.44, H, 4.85, m.p. >260°C. $^1$H-NMR: ($CDCl_3$) $\delta$ 4.60(m, 8H, $C_5H_4$), 4.30 (m, 8H, $C_5H_4$); 4.23 (s, 20H, $C_5H_5$). $^{13}$C-NMR ($CDCl_3$) $\delta$ 64.6q, 68.9, 72.0, ($C_5H_4$), 70.2 ($C_5H_5$), 86.4, 105.8 (C≡C). $^{29}$Si-NMR: ($CDCl_3$) $\delta$ −85.0. IR (KBr disk) $\nu$(C≡C) 2149 $cm^{-1}$.

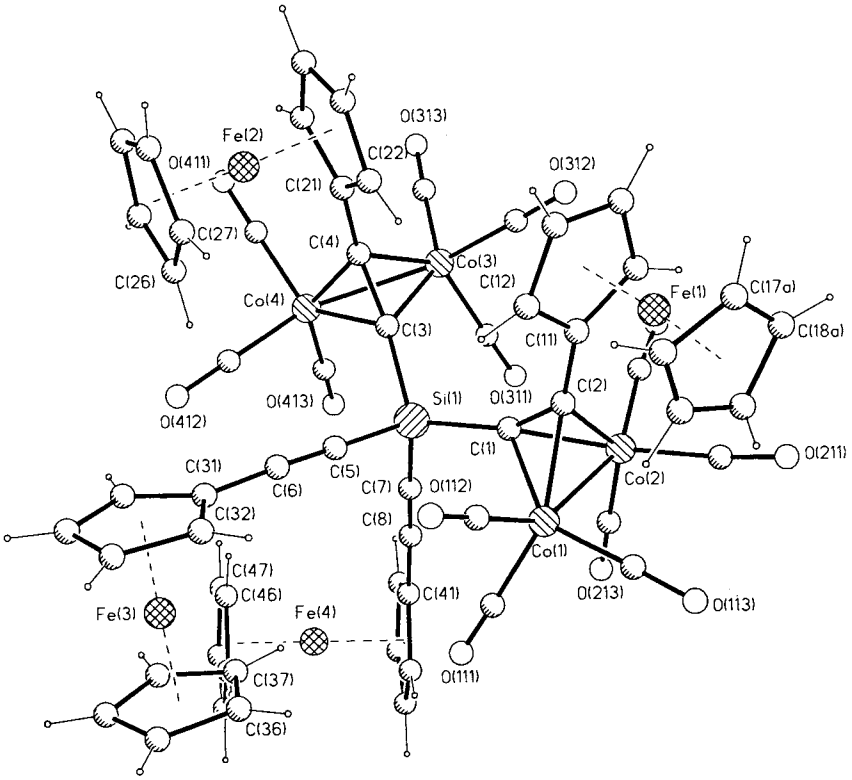


Fig. 1. Crystal structure of **20** showing the atom numbering scheme.

Three additional products separated by TLC (elutant pentane: diethyl ether). Band 1, orange oil, **8**, $[(\mu^5\text{-}C_5H_5)Fe(\mu^5\text{-}C_5H_4C_2)]Si[CH_2)_3CH_3]_3$, 37%. Anal Calcd for $C_{24}H_{36}SiFe$: C, 70.57; H, 8.88; Found C; 70.26, H, 8.84. $^1$H-NMR: ($CDCl_3$) $\delta$ 0.67 (t, 9H, $CH_3$) 0.94, 1.36–1.45 (m, 18H $(CH_2)_3$) 4.18 (m, 2H, $C_5H_4$), 4.45 (m, 2H, $C_5H_4$); 4.2 (s, 5H, $C_5H_5$). $^{13}$C-NMR ($CDCl_3$) $\delta$ 13.3, 13.9, 26.4, 26.55, ($C_4H_9$) 64.4q, 68.7, 71.9, ($C_5H_4$), 70.13 ($C_5H_5$), 88.7, 105.3 (C≡C). $^{29}$Si-NMR: ($CDCl_3$) $\delta$ −12.5. IR (KBr disk) $\nu$(C≡C) 2151 $cm^{-1}$. Band 2, **9**, $[(\eta^5\text{-}C_5H_5)Fe(\eta^5\text{-}C_5H_4C_2)]_2Si\text{-}[(CH_2)_3CH_3]_2$, 2%. *m/e* 560 ($M^+$); Anal Calcd for $C_{32}H_{36}SiFe_2$: C, 68.58; H, 6.47; Found C; 66.18, H, 6.59; m.p. 158°C. $^1$H-NMR: ($CDCl_3$) $\delta$ 0.82(m, $SiCH_2$), 0.96 (t, 6H, $CH_3$), 1.41–1.50 (m, 8H $(CH_2)_3$), 4.19 (t, 4H, $C_5H_4$), 4.48 (t, 4H, $C_5H_4$); 4.23 (s, 10H, $C_5H_5$). $^{13}$C-NMR ($CDCl_3$) $\delta$ 13.4, 14.6, 26.2, 26.3 ($C_4H_9$) 64.5q, 68.9, 71.9, ($C_5H_4$), 70.15 ($C_5H_5$), 86.4, 105.8 (C≡C). $^{29}$Si-NMR: ($CDCl_3$) $\delta$ −36.7. IR (KBr disk) $\nu$(C≡C) 2148 $cm^{-1}$. Band 3, **10**, $[(\eta^5\text{-}C_5H_5)Fe\text{-}(\eta^5\text{-}C_5H_4C_2)]_3Si[(CH_2)_3CH_3]$, 38%. $^1$H-NMR: ($CDCl_3$) $\delta$ 0.84 (m, 2H $SiCH_2$), 0.97 (t, 3H, $CH_3$), 1.43 (m, 2H $CH_2$), 1.54 (m, 2H $CH_2$), 4.21(t, 6H, $C_5H_4$), 4.50 (m, 6H, $C_5H_4$); 4.24 (s, 5H, $C_5H_5$). $^{13}$C-NMR: virtually identical to **9**. $^{29}$Si-NMR: ($CDCl_3$) $\delta$ −60.7. IR (KBr disk) $\nu$(C≡C) 2151 $cm^{-1}$.

### *3.5. Alternative preparation of $[(\eta^5\text{-}C_5H_5)Fe(\eta^5\text{-}C_5H_4C_2)]_4Si$, **11***

The previous procedure was modified to reduce by-products using 7.15mmol of FcC≡CH, 0.9 equivalent of LDA and stirring at −45°C for 1 h. A 1.0 mmol volume of $SiCl_4$ was added slowly at −78°C then the mixture was heated to 40°C. The resulting orange precipitate was recrystallised from boiling benzene yielding fine orange crystals of **11**, 87%.

### *3.6. Preparation of $[(\eta^5\text{-}C_5H_5)Fe(\eta^5\text{-}C_5H_4C(Co_2(CO)_6)C]SiPh_2Bu$, **12** and $[(\eta^5\text{-}C_5H_5)Fe(C_5H_4C(Co_2(CO)_6)C]SiMe_2Bu$ **13***

$((\eta^5\text{-}C_5H_5)Fe\text{-}(\eta^5\text{-}C_5H_4C{\equiv}C)SiR_2Bu$ (R = Ph, **1** or Me, **3**) and 2 equivalents of $Co_2(CO)_8$ were stirred for 30 min in dry hexane under nitrogen. Removal of $Co_2(CO)_8$ and solvent gave almost quantitative yields of green $[(\eta^5\text{-}C_5H_5)Fe(\eta^5\text{-}C_5H_4C(Co_2(CO)_6)C]SiPh_2Bu$, **12**, >90%. Anal Calcd for $C_{34}H_{28}O_6SiFeCO_2$: C, 55.61; H, 3.84; Found C; 55.89, H, 3.56. $^1$H-NMR: ($CDCl_3$) $\delta$ 0.88 (t, 3H, $CH_3$), 0.89 1.14 (m, 6H $(CH_2)_3$), 4.36 (m, 2H, $C_5H_4$), 4.45 (m, 2H, $C_5H_4$); 4.17 (s, 5H,$C_5H_5$) 7.45, 7.80 (m, 10H, $C_6H_5$). $^{13}$C-NMR ($CDCl_3$) $\delta$ 13.65, 15.17, 26.2, 26.6 ($C_4H_9$), 69.14, 70.77 ($C_5H_4$), 69.85 ($C_5H_5$),

Table 2
$E^0$ for ferrocenylsilanes and $Co_2(CO)_6$ derivatives

| Fc–C≡CH | **2** | **4** | **7** | **11** | Fc–X[a]–H | **16** | **17** | **4** |
|---|---|---|---|---|---|---|---|---|
| 0.61 | 0.66 | 0.66 | 0.64 | 0.62 | 0.54 | 0.56 | 0.56 | 0.61, 0.68 |

All data are referenced to ferrocene at 0.46 V, acetone, scan rate 100 mV $s^{-1}$, TEAP (0.1 M), Pt.
[a] $X = C_2Co_2(CO)_6$.

128.0 (C≡C), 130.1, 135.6 ($C_6H_5$), 198 (CO). $^{29}$Si-NMR: ($CDCl_3$) $\delta$ −4.3. IR (KBr disk) $\nu$(C≡O) 2083(s), 2051(vs), 2019(vs) $cm^{-1}$, and green [($\eta^5$-$C_5H_5$)Fe($\eta^5$-$C_5H_4C(Co_2(CO)_6)C$]-$SiMe_2Bu$, **13** >90%. Anal Calcd for $C_{24}H_{24}O_6SiFeCO_2$: C, 47.24; H, 3.96; Found C; 47.34, H, 3.70. $^1$H-NMR: ($CDCl_3$) $\delta$ 0.96, 0.99, 1.02, 1.51 ($CH_3$ and $CH_2$), 4.37 (m, 2H, $C_5H_4$), 4.45 (m, 2H, $C_5H_4$), 4.19 (s, 5H, $C_5H_5$). $^{29}$Si-NMR: ($CDCl_3$): $\delta$ 1.31. IR (KBr disc): 2081s, 2047vs, 2014vs $\nu$(C≡O) $cm^{-1}$.

Similar reactions between a slight molar excess of $Co_2(CO)_8$ and **2**, **4**, **7**, and **11** gave the following products. From **2**: green, [($\eta^5$-$C_5H_5$)Fe($\eta^5$-$C_5H_4C(Co_2(CO)_6)C$]$SiPh_2$(C≡C-$\eta^5$-$C_5H_4$)Fe($\eta^5$-$C_5H_5$), **14**, <1%. *m/e* 830 [(M-2CO)$^+$] IR (KBr disk): $\nu$(C≡C) 2150; $\nu$(C≡O) 2083(s), 2049(vs), 2020(vs) $cm^{-1}$, and green, [($\eta^5$-$C_5H_5$)Fe($\eta^5$-$C_5H_4C(Co_2(CO)_6)$-C]$_2SiPh_2$, **16**, 75%. *m/e* 1088 [(M-3CO)$^+$]. Anal Calcd for $C_{48}H_{28}O_{12}SiFe_2CO_4$: C, 49.18; H, 2.41; Found C; 49.84, H, 2.33. $^1$H-NMR: ($CDCl_3$) 4.42 (m, 4H, $C_5H_4$), 4.69 (m, 4H, $C_5H_4$); 4.32 (s, 10H, $C_5H_5$) 7.47, 8.09 (m, 10H, $C_6H_5$). $^{13}$C-NMR ($CDCl_3$) $\delta$ 68.9q, 69.2, 70.1, 72.0 ($C_5H_4$), 69.85 ($C_5H_5$), 128.1 (C≡C), 130.4, 135.3 ($C_6H_5$), 201 (CO). $^{29}$Si-NMR: ($CDCl_3$) $\delta$ −29.8, IR (KBr disc) $\nu$(C≡O): 2079(s), 2049(vs), 2016(vs) $cm^{-1}$. From **4**: green [($\eta^5$-$C_5H_5$)Fe($\eta^5$-$C_5H_4C(Co_2(CO)_6)C$]$SiMe_2$(C≡C-$\eta^5$-$C_5H_4$)Fe($\eta^5$-$C_5H_5$), **15**, <1%. 14, <1%. *m/e* 706 [(M-2CO)$^+$] IR (KBr disk) $\nu$(C≡C) 2149; $\nu$(C≡O) 2089(s), 2052(vs), 2025(vs) $cm^{-1}$, and green [($\eta^5$-$C_5H_5$)Fe($\eta^5$-$C_5H_4C$-$(Co_2(CO)_6)C]_2SiMe_2$, **17**, 60%. *m/e* 964 [(M-3CO)$^+$], Anal Calcd for $C_{38}H_{24}O_{12}SiFe_2CO_4$: C, 43.55; H, 2.31; Found C; 43.80, H, 2.14. $^1$H-NMR: ($CDCl_3$) $\delta$ 0.80 (s, 6H, $CH_3$) 4.36 (m, 4H, $C_5H_4$), 4.49 (m, 4H, $C_5H_4$); 4.22 (s, 10H, $C_5H_5$). $^{13}$C-NMR ($CDCl_3$) $\delta$ 0.21 ($CH_3$) 68.7q, 69.0, 69.9, 71.9 ($C_5H_4$), 69.86 ($C_5H_5$), 200 (CO). IR (KBr disk) $\nu$(C≡O) 2081(s), 2050(vs), 2020(vs) $cm^{-1}$. From **7**: green, [($\eta^5$-$C_5H_5$)Fe($\eta^5$-$C_5H_4C(Co_2(CO)_6)C$]SiMe[(C≡C-$\eta^5$-$C_5H_4$)Fe($\eta^5$-$C_5H_5$)]$_2$, **18**, <1%. *m/e* 872 [(M-3CO)$^+$] IR (KBr disk) $\nu$(C≡C) 2148; $\nu$(C≡O) 2059(s), 2050(vs), 2018(vs) $cm^{-1}$, and green **19**, [($\eta^5$-$C_5H_5$)Fe($\eta^5$-$C_5H_4C$-$(Co_2(CO)_6)C]_2$-SiMe[(C≡C-$\eta^5$-$C_5H_4$)Fe($\eta^5$-$C_5H_5$)], 60%. *m/e* 1186 [(M-2CO)$^+$], Anal Calcd for $C_{49}H_{30}O_{12}SiFe_3CO_4$: C, 47.38; H, 2.43; Found C; 47.52, H, 2.30. $^1$H-NMR: ($CDCl_3$) 0.98 (s, 6H, $CH_3$) 4.21, 4.34, 4.48, 4.64 (m, 12H, $C_5H_4$); 4.24 (s, 10H, $C_5H_5$); 4.27 (s, 5H, $C_5H_5$). $^{13}$C-NMR ($CDCl_3$) $\delta$ 4.59 ($CH_3$) 68.59, 68.61, 69.06, 70.03, 71.46, 71.6, 71.65 ($C_5H_4$), 69.1, 70,0 ($C_5H_5$), 105.8 (C≡C) 200 (CO). $^{29}$Si-NMR: ($CDCl_3$) $\delta$ −32.9, IR (KBr disk) $\nu$(C≡C) 2150; $\nu$(C≡O) 2083(s), 2051 (vs), 2019(vs) $cm^{-1}$. In an attempt to force further substitution a 10-fold excess of $Co_2(CO)_8$ was employed and the solution refluxed in benzene for 1 h. TLC revealed the presence of $Co_2(CO)_8$, $Co_4(CO)_{12}$ and **19**. There was no evidence of a tris-substituted complex.

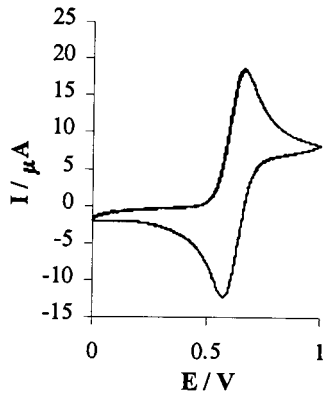


Fig. 2. Cyclic voltammogram of **7** at 100 mV $s^{-1}$.

### 3.7. Preparation of [($\eta^5$-$C_5H_5$)Fe($\eta^5$-$C_5H_4C(Co_2(CO)_6)C]_2Si$-[C≡C($\eta^5$-$C_5H_4$)Fe($\eta^5$-$C_5H_5$)]$_2$, **20**

Typically a 5-fold excess of $Co_2(CO)_8$ was added to a suspension of **11** in hexane and stirred for 30 min. Excess $Co_2(CO)_8$ was removed by elution with hexane and a single, dark green product band was eluted with diethyl ether. The resulting product was crystallised from benzene/pet. ether (40–60°) to yield [($\eta^5$-

Table 3
$\Delta E_{1/2}$ values for some bis-ferrocenyl compounds

| Compound | $\Delta E_{1/2}$ (mV) |
|---|---|
| Fc–Fc [28] | 350 |
| Fc–C≡C–Fc [29] | 130 |
| Fc–(C≡C)$_2$–Fc [30] | 100 |
| Fc–$SiMe_2$Fc [5,30,31] | 150 |
| Fc–($SiMe_2$)$_2$–Fc [5] | 110 |
| Fc–($SiMe_2$)$_3$–Fc [5] | 80 |
| (FcC≡C)$_{4-n}SiR_n$ | <30 |

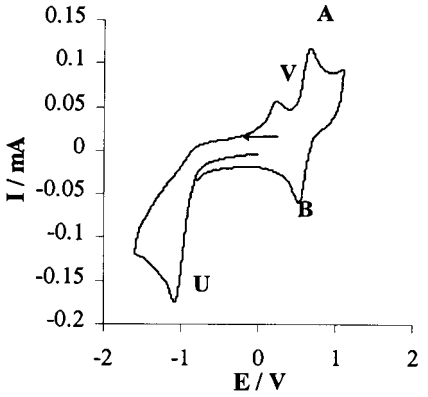


Fig. 3. Cyclic voltammogram of **16** at 400 mV $s^{-1}$.

$C_5H_5$)Fe($\eta^5$-$C_5H_4$C-($Co_2(CO)_6$)C]$_2$Si[(C≡C-$\eta^5$-$C_5H_4$)Fe-($\eta^5$-$C_5H_5$)]$_2$, **20**, 75%. *m/e* 1352 [(M-3CO)$^+$], Anal Calcd for $C_{60}H_{36}O_{12}SiFe_4CO_4$: C, 50.18; H, 2.53; Found C; 50.29, H, 2.37. $^1$H-NMR: ($CDCl_3$) $\delta$ 4.22,4.28, 4.35, 4.36, 4.44, 4.50, 4.65, 4.90 (m, 16H, $C_5H_4$); 4.20, 4.25 (s, 10H, $C_5H_5$); 4.26, 4.29 (s, 10H, $C_5H_5$). $^{13}$C-NMR ($CDCl_3$) $\delta$ 68.44q, 68.94, 69.20, 70.40, 71.80, 72.10q ($C_5H_4$), 69.2, 70.4 ($C_5H_5$), 199 (CO). IR (KBr disk) $\nu$(C≡O) 2087(s), 2054(vs), 2019(vs) $cm^{-1}$ Several reactions were attempted to increase the degree of complexation (changing solvents i.e. benzene, THF) and reaction conditions (refluxing for 4 h, or stirring 72 h) without success.

### 3.8. X-ray structure analysis

Diffraction data were collected on a black, irregular plate-like crystal of 20 on a Nicolet R3M diffractometer using graphite modulated Mo–$K_\alpha$ radiation at 132 K. The crystals were weakly diffracting with less than 50% of the 8996 independent reflections, collected out to $2\theta = 48°$, having $I > 2\sigma(I)$. The data were corrected for Lorentz and polarisation effects and empirical absorption corrections applied using SHELXTL [35]. Details of the crystal, data collection and refinement are summarised in Table 4. The structure was solved by direct methods using SHELXS-86 [36]. The optimum E-map revealed the location of the Fe, Co, Si and several of the C and O atoms. The remaining non-hydrogen atoms found in subsequent least squares refinement, difference Fourier cycles. Weighted full matrix refinement on $F_o^2$ was performed using SHELXL-93 [37]. All nonhydrogen atoms were refined with anisotropic temperature factors and hydrogen atoms were included in calculated positions using a riding model. A difference synthesis following the location of all nonhydrogen atoms revealed the presence of a methanol solvate, disordered about an inversion centre. Significant improvement in the overall model was obtained with the C and O atoms of the solvate refined isotropically with half occupancy. H atoms were included on the methyl C atom of the solvate but the O–H hydrogen atom was not assigned. High and increasing temperature factors for the C(16)–C(18) atoms of the free cyclopentadiene ring bound to Fe(l) indicated positional disorder. This was modelled by assigning alternative locations for each of the C atoms and refinement of their occupancy factors converged at 0.53(4) for C(16A)–C(18A) and 0.47(4) for C(16B)–C(18B). Hydrogen atoms were included in calculated positions on

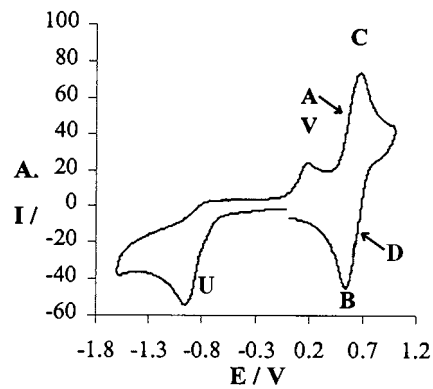


Fig. 4. Cyclic voltammogram of **20** at 200 mV $s^{-1}$.

Table 4
Crystal data and structure refinement for **20**

| | |
|---|---|
| Empirical formula | $C_{60.5}H_{37.5}Co_4Fe_4O_{12.5}Si$ |
| Formula weight | 1451.61 |
| Temperature (K) | 132(2) |
| Wavelength (Å) | 0.71073 |
| Crystal system | Monoclinic |
| Space group | $P2_1/c$ |
| Unit cell dimensions | |
| $a$ (Å) | 12.039(7) |
| $b$ (Å) | 13.996(7) |
| $c$ (Å) | 34.673(3) |
| $\beta$ (°) | 98.98(5) |
| Volume (Å$^3$) | 5771(4) |
| $Z$ | 4 |
| $D_{calc}$ (Mg $m^{-3}$) | 1.671 |
| Absorption coefficient ($mm^{-1}$) | 2.179 |
| Transmission coefficient | 1.000(max), 0.619(min) |
| $F(000)$ | 2906 |
| Crystal size (mm) | $0.80 \times 0.76 \times 0.24$ |
| $\theta$ range for data collection (°) | 2.23–23.99 |
| Index ranges | $0 \le h \le 13$; $0 \le k \le 15$; $-39 \le 1 \le 39$ |
| Reflections collected | 9480 |
| Independent reflections | 8996 [$R_{int} = 0.0745$] |
| Refinement method | Full-matrix least-squares on $F^2$ |
| Data/restraints/parameters | 8996/0/737 |
| Goodness-of-fit on $F^2$ | 1.042 |
| Final $R$ indices [$I > 2\sigma(I)$] | $R_1^a = 0.0783$, $wR_2 = 0.1505$ |
| $R$ indices (all data) | $R_1 = 0.1917$, $wR_2 = 0.1940$ |
| Largest diff. peak and hole (e Å$^{-3}$) | 1.045 and −0.640 |

[a] $R_1 = (\Sigma||F_o| - |F_c||/\Sigma|F_o|)$; $wR_2 = [\Sigma\omega(F_o^2 - F_c^2)^2/\Sigma\omega F_o^4]^{1/2}$.

Table 5
Atomic coordinates [$\times 10^4$] and equivalent isotropic displacement parameters [$Å^2 \times 10^3$] for **20**

| | $x$ | $y$ | $z$ | $U_{eq}$ |
|---|---|---|---|---|
| Si(l) | −1462(3) | 5471(3) | 1347(1) | 25(1) |
| C(1) | −2020(10) | 6606(8) | 1142(3) | 23(3) |
| C(2) | −2892(11) | 7135(9) | 978(3) | 29(3) |
| Co(l) | −2113(1) | 7779(1) | 1450(1) | 30(1) |
| C(111) | −816(12) | 7683(10) | 1815(4) | 39(4) |
| O(111) | −57(8) | 7616(7) | 2037(3) | 57(3) |
| C(112) | −3095(12) | 7479(10) | 1760(4) | 37(4) |
| O(112) | −3737(8) | 7294(7) | 1964(3) | 44(3) |
| C(113) | −2398(10) | 9012(10) | 1403(3) | 29(3) |
| O(113) | −2553(8) | 9846(7) | 1375(3) | 46(3) |
| Co(2) | −1525(1) | 7622(1) | 804(1) | 33(1) |
| C(211) | −2055(12) | 8734(12) | 599(4) | 41(4) |
| O(211) | −2444(9) | 9415(7) | 446(3) | 55(3) |
| C(212) | −1417(12) | 7024(10) | 356(5) | 43(4) |
| O(212) | −1319(9) | 6710(7) | 60(3) | 56(3) |
| C(213) | −51(13) | 7764(11) | 981(4) | 49(4) |
| O(213) | 885(8) | 7865(8) | 1103(3) | 71(4) |
| C(11) | 4049(10) | 6992(8) | 786(3) | 23(3) |
| C(12) | −4959(10) | 6677(10) | 971(4) | 42(4) |
| C(13) | −5892(12) | 6531(11) | 681(4) | 49(4) |
| C(14) | −5558(12) | 6737(10) | 319(4) | 49(4) |
| C(15) | −4457(11) | 7070(10) | 386(4) | 40(4) |
| Fe(l) | −5406(2) | 7908(2) | 675(1) | 41(1) |
| C16A | −6430(4) | 8660(3) | 995(15) | 72(14) |
| C17A | −6660(4) | 8840(3) | 598(15) | 69(15) |
| C18A | −5850(4) | 9200(3) | 442(14) | 65(12) |
| C16B | −6820(3) | 8640(3) | 736(14) | 42(13) |
| C17B | −6520(3) | 8870(3) | 349(13) | 53(13) |
| C18B | −5380(4) | 9230(3) | 366(12) | 52(13) |
| C(19) | −4993(14) | 9304(12) | 763(6) | 60(5) |
| C(110) | −5520(2) | 8988(16) | 1046(7) | 103(8) |
| C(3) | −1751(10) | 4422(9) | 1034(3) | 25(3) |
| C(4) | −2416(10) | 3706(9) | 886(3) | 24(3) |
| Co(3) | −1397(2) | 4117(1) | 511(1) | 32(1) |
| C(311) | −122(12) | 4814(10) | 513(4) | 41(4) |
| O(311) | 688(8) | 5221(7) | 502(3) | 52(3) |
| C(312) | −2437(12) | 4805(10) | 212(4) | 36(4) |
| O(312) | −3128(9) | 5242(7) | 28(3) | 60(3) |
| C(313) | −1291(11) | 3150(11) | 185(4) | 42(4) |
| O(313) | −1207(9) | 2545(7) | −29(3) | 57(3) |
| Co(4) | −962(1) | 3177(1) | 1116(1) | 31(1) |
| C(411) | −1182(12) | 1977(11) | 952(4) | 44(4) |
| O(411) | −1385(9) | 1201(7) | 850(3) | 56(3) |
| C(412) | −1024(11) | 3042(10) | 1624(5) | 43(4) |
| O(412) | −1023(8) | 2941(8) | 1954(3) | 55(3) |
| C(413) | 540(13) | 3369(10) | 1153(4) | 45(4) |
| O(413) | 1485(8) | 3462(7) | 1173(3) | 62(3) |
| C(21) | −3574(10) | 3397(10) | 803(4) | 37(4) |
| C(22) | −4525(11) | 3986(10) | 832(4) | 40(4) |
| C(23) | −5478(12) | 3404(13) | 703(5) | 57(5) |
| C(24) | −5161(14) | 2514(14) | 595(4) | 62(5) |
| C(25) | −3956(13) | 2484(11) | 664(4) | 48(4) |
| Fe(2) | −4552(2) | 2784(1) | 1165(1) | 30(1) |
| C(26) | −3839(11) | 2897(10) | 1741(4) | 34(3) |
| C(27) | −4985(11) | 3127(11) | 1695(4) | 41(4) |
| C(28) | −5597(11) | 2311(12) | 1529(4) | 47(4) |
| C(29) | −4818(14) | 1605(11) | 1473(4) | 55(5) |
| C(210) | −3735(11) | 1973(10) | 1602(4) | 35(4) |
| C(5) | −2067(10) | 5278(9) | 1782(4) | 26(3) |
| C(6) | −2419(10) | 5098(9) | 2081(4) | 34(3) |
| C(31) | −2730(10) | 4872(9) | 2452(3) | 23(3) |

Table 5 (Continued)

| | $x$ | $y$ | $z$ | $U_{eq}$ |
|---|---|---|---|---|
| C(32) | −3411(9) | 5439(10) | 2667(4) | 37(4) |
| C(33) | −3446(11) | 4954(10) | 3030(4) | 41(4) |
| C(34) | −2830(12) | 4090(11) | 3021(4) | 45(4) |
| C(35) | −2395(11) | 4044(9) | 2677(4) | 36(4) |
| Fe(3) | −1843(2) | 5241(1) | 2973(1) | 31(1) |
| C(36) | −1142(12) | 6525(12) | 3046(7) | 78(7) |
| C(37) | −472(12) | 5939(11) | 2861(5) | 51(4) |
| C(38) | −147(11) | 5178(11) | 3098(5) | 50(4) |
| C(39) | −604(13) | 5257(15) | 3441(5) | 71(6) |
| C(310) | −1196(16) | 6126(16) | 3411(7) | 87(7) |
| C(7) | 23(10) | 5584(10) | 1478(4) | 34(3) |
| C(8) | 1016(12) | 5718(8) | 1579(4) | 29(3) |
| C(41) | 2215(11) | 5881(10) | 1722(4) | 36(4) |
| C(42) | 2618(12) | 6529(10) | 2023(5) | 58(5) |
| C(43) | 3798(11) | 6455(11) | 2082(5) | 51(4) |
| C(44) | 4125(11) | 5757(10) | 1838(4) | 40(4) |
| C(45) | 3152(10) | 5388(10) | 1610(4) | 38(4) |
| Fe(4) | 3078(1) | 5181(1) | 2185(1) | 30(1) |
| C(46) | 2927(12) | 3782(11) | 2281(4) | 46(4) |
| C(47) | 2000(11) | 4254(11) | 2376(4) | 42(4) |
| C(48) | 2370(12) | 4897(13) | 2665(5) | 58(5) |
| C(49) | 3569(12) | 4832(11) | 2751(4) | 45(4) |
| C(410) | 3917(12) | 4111(10) | 2511(4) | 42(4) |
| C(1S) | 1000(2) | 819(19) | 370(8) | 40(7) |
| O(1S) | 480(2) | 20(2) | 155(8) | 100(9) |

$U_{eq}$ is defined as one third of the trace of the orthogonalized $U_{ij}$ tensor.

these disordered C atoms. This model of the structure converged with $R = 0.0783$ and $wR_2 = 0.1917$. Final positional and equivalent thermal parameters are given in Table 5.

## 4. Supplementary material

Full bond length tables together with tables of thermal parameters, hydrogen atom parameters and observed and calculated structure factors for both structures can be obtained from the authors (JS).

## References

[1] (a) C. Levanda, K. Beckgaard, D.O. Cowan, M.D. Rausch, J. Org. Chem. 41 (1976) 2700. (b) S. Barlow, D O'Hare, Chem. Rev. 97 (1997) 637.
[2] N.W. Duffy, C.J. McAdam, C. Nervi, D. Osella, M. Ravera, B.H. Robinson, J. Simpson, Inorg. Chim. Acta 247 (1996) 99.
[3] C.J. McAdam, N.W. Duffy, B.H. Robinson, J. Simpson, Organometallics (1996) 3935.
[4] (a) Z. Yuan, N.J. Taylor, Y. Sun, T.B. Marder, J. Organomet. Chem. 449 (1993) 27. (b) M.C.B. Colbert, S.L. Ingham, J. Lewis, N.J. Long, P.R. Raithby, J. Chem. Soc. Dalton Trans. (1994) 2215. (c) M. Sato, E. Mogi, S. Kumakura, Organometallics 14 (1995) 3157. (d) M.C.B. Colbert, D. Hodgson, J. Lewis, P.R. Raithby, Polyhedron 14 (1995) 2759. (e) S.L. Ingham, M.S. Khan, J. Lewis, N.J. Long, P.R. Raithby, J. Organomet. Chem. 470 (1994) 153.

[5] V.V. Dement'ev, F. Cervantes-Lee, L. Parkanyi, H. Sharma, K.H. Pannell, M.T. Nguyen, A. Diaz, Organometallics 12 (1993) 1983.
[6] D.L. Zechel, D.A. Foucher, J.K. Pudelski, G.P.A. Yap, A.L. Rheingold, I Manners, J. Chem. Soc. Dalton Trans. (1995) 1893.
[7] J. Park, Y. Seo, S. Cho, D. Whang, K. Kim, T. Chang, J. Organomet. Chem 489 (1995) 23.
[8] B.Z. Tang, R. Petersen, D.A. Foucher, A. Lough, N. Coombs, R. Sodhi, I Manners, J. Chem. Soc. Chem. Commun (1993) 523.
[9] D.A. Foucher, C.H. Honeyman, J.M. Nelson, B.Z. Tang, I. Manners, Angew. Chem. Int. Ed. Engl. 32 (1993) 1709.
[10] M.T. Nguyen, A. Diaz, V.V. Dement'ev, K.H. Pannell, Chem. Mater. 5 (1993) 1389.
[11] D.A. Foucher, B.Z. Tang, I Manners, J. Am. Chem. Soc. 114 (1992) 6246.
[12] C. Eisenbroch, A. Bretschneider-Hurley, J. Hurley, A. Behrendt, W. Massa, S. Wocadlo, E. Reijerse, Inorg. Chem. 34 (1995) 743.
[13] J. Borgdorf, E.J. Ditzel, N.W. Duffy, B.H. Robinson, J. Simpson, J. Organomet. Chem. 437 (1992) 323.
[14] J. Borgdorf, N.W. Duffy, B.H. Robinson, J. Simpson, Inorg. Chim.Acta 224 (1994) 73.
[15] L.P. Asatiani, D.S. Zurabishvili, I.M. Gverdsiteli, Zh. Obshch. Khim. 45 (1973) 577.
[16] R.K. Harris, J.D. Kennedy, W. McFarlane, in: R.K. Harris, B.E. Mann (Eds.), NMR and the Periodic Table, Academic Press, London, 1978, p. 309.
[17] E.A. Williams, J.D. Gargioli, in: G.A. Webb (Ed.), Annual Reports on NMR Spectroscopy, vol. 9, Academic Press, London, 1979.
[18] R.S. Dickson, P.J. Fraser, Adv. Organomet. Chem. 12 (1974) 323.
[19] R.J.P. Corriu, J.J.E. Moreau, H. Praet, J. Organomet. Chem. 376 (1989) 39.
[20] B. Happ, T. Bartik, C. Zucchi, M.C. Rossi, F. Ghelfi, G. Palyi, G. Varadi, G. Szalontai, I.T. Horvath, A. Chiesi-Villa, C. Guastini, Organometallics 14 (1995) 809.
[21] M. Nardelli, PARST: a system for calculating molecular structure parameters from diffraction data, Comput. Chem. 7 (1983) 95.
[22] C.M. Arewgoda, B.H. Robinson, J. Simpson, J. Am. Chem. Soc. 105 (1983) 1893.
[23] B.M. Peake, P.H. Rieger, B.H. Robinson, J. Simpson, J. Am. Chem. Soc. 102 (1980) 156.
[24] D.M. Hoffmann, R. Hoffmann, C.R. Fisel, J. Am. Chem. Soc. 104 (1982) 3858.
[25] D. Gregson, J.A.K. Howard, Acta Crystallogr. C39 (1983) 1024.
[26] B.F.G Johnson, J. Lewis, P.R. Raithby, D.A. Wilkinson, J. Organomet. Chem. 408 (1991) C9.
[27] J.B. Flanagan, S. Margel, A.J. Bard, F.C. Anson, J. Am. Chem. Soc. 100 (1978) 4248.
[28] G.M. Brown, T.J. Meyer, D.O. Cowan, C. Levanda, F. Kaufman, P.V. Roling, M.D. Rausch, Inorg. Chem. 14 (1975) 506.
[29] C. Levanda, K. Bechgaard, D.O. Cowan, J. Org. Chem. 41 (1976) 2700.
[30] R. Rulkens, A.J. Lough, I Manners, J. Am. Chem. Soc. 116 (1994) 797.
[31] A.B. Bocarsly, E.G. Walton, M.G. Bradley, M.S. Wrighton, J. Electroanal. Chem. Interfac. Electrochem. 100 (1979) 283.
[32] B.M. Peake, P.H. Rieger, B.H. Robinson, J. Simpson, S.V. Visco, J. Am. Chem. Soc. 104 (1982) 5633.
[33] G. Balvoine, G. Doisneau, T. Fillebeen-Khan, J. Organomet. Chem. 425 (1992) 113.
[34] M. Applebaum, M. Rosenblum, N. Brawn, J. Papenmeier, J. Organomet. Chem. 6 (1966) 173.
[35] G.M. Sheldrick, SHELXTL, an integrated system for solving, refining and displaying crystal structures from diffraction data. University of Göttingen, Göttingen, 1981.
[36] G.M. Sheldrick, SHELXS-86, program for the solution of crystal structures from diffraction data. University of Göttingen, Göttingen, 1986.
[37] G.M. Sheldrick, SHELXL-93; A program for the refinement of crystal structures from diffraction data. University of Göttingen, Göttingen, 1993.